REPORT 1361

APPROXIMATE ANALYSIS OF EFFECTS OF LARGE DEFLECTIONS AND INITIAL TWIST ON TORSIONAL STIFFNESS OF A CANTILEVER PLATE SUBJECTED TO THERMAL STRESSES [1]

By Richard R. Heldenfels and Louis F. Vosteen

SUMMARY

An approximate analysis of the nonlinear effects of initial twist and large deflections on the torsional stiffness of a cantilever plate subjected to a nonuniform temperature distribution is presented. The Von Kármán large-deflection equations are satisfied through the use of a variational principle. The results show that initial twist and applied moments can have significant effects on the changes in stiffness produced by nonuniform heating, particularly in the region of the buckling temperature difference. Results calculated by this approximate analysis are in satisfactory agreement with measured torsional deformations and changes in natural frequency.

INTRODUCTION

One of the structural problems of high-speed flight is the reduction of effective stiffness of structures due to the thermal stresses produced by aerodynamic heating. A reduction in torsional stiffness can be an important factor in aeroelastic problems as indicated in references 1 and 2. A similar reduction in stiffness produced by thermal stresses presumably caused the flutter and failures of some structural models described in reference 3. A simple method for calculating the reduction in torsional stiffness of thin wings is presented in reference 4. In reference 5 the results calculated from a small-deflection plate theory are compared with experimentally determined changes in the torsional stiffness of a cantilever plate rapidly heated along the longitudinal edges. The theory used in reference 5 predicted the general effect of thermal stresses on the torsional stiffness, as indicated by measurements of torsional deformation and changes in natural frequency of vibration, but overestimated the magnitude of the changes.

The purpose of this paper is to present the results of an approximate analysis to show that the differences between theory and experiment noted in reference 5 are due to the nonlinear effects of large deflections and initial deformations not included in the small-deflection analysis. The analytical approach used to account for large deflections and initial deformations is presented, the general significance of the results is discussed, and calculated values are compared with the experimental data of reference 5.

SYMBOLS

a	plate length in x-direction
$A_1, A_2, \ldots A_i$	coefficients of series expansion for plate deflection
b	half-plate width in y-direction
C	coefficient of stress function
D	plate flexural stiffness, $\frac{Et^3}{12(1-\mu^2)}$
E	modulus of elasticity
F	stress function defining stress distribution in plate
$f_1, f_2, \ldots f_i$	selected functions of x and y
$I_1, I_2, \ldots I_i$	values obtained from definite integrals
GJ	torsional stiffness
$(GJ)_0$	torsional stiffness of flat, unstressed plate
$\Delta(GJ)$	incremental torsional stiffness
$\Delta(GJ)_i$	initial incremental torsional stiffness before heating
$\Delta(GJ)_{min}$	minimum incremental torsional stiffness
m	nondimensional moment
M	applied moment (positive in direction of positive twist)
p	pressure
t	plate thickness
T	temperature
ΔT	particular temperature difference
ΔT_{cr}	critical value of ΔT
w	total plate deflection
w_i	initial plate deflection
x,y	coordinate axes
α	coefficient of thermal expansion
ϵ	small dynamic perturbation
ζ	exponential parameter of temperature distribution function
θ	twist at plate tip
θ_i	initial twist at plate tip
λ	temperature ratio, $\Delta T/\Delta T_{cr}$
λ_{min}	value of λ corresponding to $\Delta(GJ)_{min}$
μ	Poisson's ratio
ρ	density

[1] Supersedes NACA Technical Note 4067 by Richard R. Heldenfels and Louis F. Vosteen, 1957.

σ_x, σ_y	normal stresses in plane of plate in x- and y-directions, respectively, positive for tension
τ_{xy}	shear stress in plane of plate
τ	time
φ	nondimensional twist
φ_i	initial nondimensional twist
ω	circular frequency
ω_0	circular frequency of unheated perfect plate
ω_i	initial circular frequency
ω_{min}	minimum circular frequency
∇^2	differential operator, $\frac{\partial^2}{\partial x^2}+\frac{\partial^2}{\partial y^2}$
∇^4	differential operator, $\frac{\partial^4}{\partial x^4}+2\frac{\partial^4}{\partial x^2\partial y^2}+\frac{\partial^4}{\partial y^4}$

Double dot indicates second derivative with respect to time.

ANALYSIS

STATEMENT OF PROBLEM

The studies presented herein are primarily concerned with the twist of a uniformly thick rectangular cantilever plate shown in figure 1. The equations are derived to consider the effects of initial twist, applied moments, and thermal stresses on the torsional deformations and natural frequencies of plates. The analysis involves an approximate solution of the Von Kármán large-deflection equations which have been modified to include the effects of initial imperfections and nonuniform temperature distributions. The modified equations are (from ref. 6)

$$\nabla^4 F=-E\alpha\nabla^2 T+E\left[\left(\frac{\partial^2 w}{\partial x\,\partial y}\right)^2-\frac{\partial^2 w}{\partial x^2}\frac{\partial^2 w}{\partial y^2}-\left(\frac{\partial^2 w_i}{\partial x\,\partial y}\right)^2+\frac{\partial^2 w_i}{\partial x^2}\frac{\partial^2 w_i}{\partial y^2}\right] \tag{1a}$$

$$\nabla^4(w-w_i)=\frac{p}{D}+\frac{t}{D}\left(\frac{\partial^2 F}{\partial y^2}\frac{\partial^2 w}{\partial x^2}+\frac{\partial^2 F}{\partial x^2}\frac{\partial^2 w}{\partial y^2}-2\frac{\partial^2 F}{\partial x\,\partial y}\frac{\partial^2 w}{\partial x\,\partial y}\right) \tag{1b}$$

where F is the stress function such that

$$\sigma_x=\frac{\partial^2 F}{\partial y^2} \tag{2a}$$

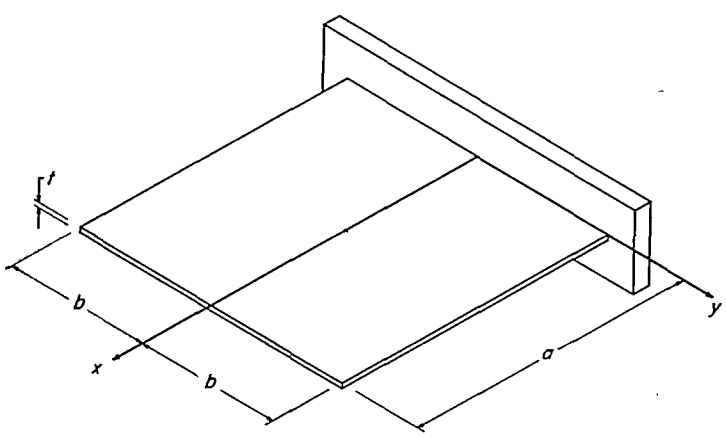

FIGURE 1.—Dimensions and coordinate system of cantilever plate.

$$\sigma_y=\frac{\partial^2 F}{\partial x^2} \tag{2b}$$

$$\tau_{xy}=-\frac{\partial^2 F}{\partial x\,\partial y} \tag{2c}$$

Equation (1a) is the differential equation for compatibility in the plane of the plate and equation (1b) is the differential equation for equilibrium of forces acting perpendicular to the plane of the plate. The solution of equations (1), subject to the proper boundary conditions on the deflections and stresses, describes the behavior of the plate under the applied loads p and the temperature distribution T. For the purpose of this paper the assumption is made that no external loads are applied in the plane of the plate so that the inplane stresses defined by the stress function F are zero at the free boundaries (stress-free edges). Equations (1) apply to both the dynamic and the static problem if p includes the dynamic loads as well as static loads.

APPROXIMATE SOLUTION OF EQUATIONS

Exact solutions of the Von Kármán large-deflection equations are difficult to obtain, but approximate solutions can be obtained to any desired accuracy by several methods. For the analysis herein equations (1) will be satisfied through the use of the following variational principle:

$$\delta\Bigg(\iint\frac{D}{2}\left\{[\nabla^2(w-w_i)]^2-2(1-\mu)\left[\frac{\partial^2(w-w_i)}{\partial x^2}\frac{\partial^2(w-w_i)}{\partial y^2}-\left(\frac{\partial^2(w-w_i)}{\partial x\,\partial y}\right)^2\right]\right\}dx\,dy+\iint\frac{t}{2}\left\{\frac{\partial^2 F}{\partial y^2}\left[\left(\frac{\partial w}{\partial x}\right)^2-\left(\frac{\partial w_i}{\partial x}\right)^2\right]+\frac{\partial^2 F}{\partial x^2}\left[\left(\frac{\partial w}{\partial y}\right)^2-\left(\frac{\partial w_i}{\partial y}\right)^2\right]-2\frac{\partial^2 F}{\partial x\,\partial y}\left(\frac{\partial w}{\partial x}\frac{\partial w}{\partial y}-\frac{\partial w_i}{\partial x}\frac{\partial w_i}{\partial y}\right)\right\}dx\,dy-\iint\frac{t}{2E}\left[\left(\frac{\partial^2 F}{\partial x^2}\right)^2+\left(\frac{\partial^2 F}{\partial y^2}\right)^2-2\mu\frac{\partial^2 F}{\partial x^2}\frac{\partial^2 F}{\partial y^2}+2(1+\mu)\left(\frac{\partial^2 F}{\partial x\,\partial y}\right)^2\right]dx\,dy-\iint t\alpha T\left(\frac{\partial^2 F}{\partial x^2}+\frac{\partial^2 F}{\partial y^2}\right)dx\,dy-\iint p(w-w_i)dx\,dy\Bigg)=0 \tag{3}$$

This principle is essentially a particularization of one given by Reissner (ref. 7) and also has been modified to include the effects of initial deformations and a nonuniform temperature distribution. The deflection w must satisfy the geometrical boundary conditions, that is, the conditions imposed on slopes and deflections. Variation of equation (3) with respect to F yields equation (1a) and the associated natural boundary conditions, and variation with respect to w yields equation (1b) and the associated natural boundary conditions.

The following assumptions for stress, deflection, and temperature are made:

$$\left.\begin{aligned} F&=Cf_1\\ w&=b\theta f_2\\ w_i&=b\theta_i f_2\\ T&=\Delta T f_3\end{aligned}\right\} \tag{4}$$

where the stress coefficient C and the tip twist θ are to be determined by means of the variational principle. The functions f_1, f_2, and f_3, the initial tip twist θ_i, and the temperature coefficient ΔT are presumed to be known. Selection of these quantities is discussed in appendix A. It should be noted here that, although the temperature distribution is considered to vary with time, the shapes of the plate deflection and of the stress function are assumed to remain constant during heating or loading.

The unknown coefficient of the stress function C is obtained by substituting equations (4) into equation (3) and taking the variation with respect to C. The result is

$$C=-E\alpha\,\Delta T\left(\frac{I_2}{I_1}\right)+Eb^2(\theta^2-\theta_i^2)\left(\frac{I_3}{I_1}\right) \tag{5}$$

where

$$I_1=\iint\left[\left(\frac{\partial^2 f_1}{\partial y^2}\right)^2+\left(\frac{\partial^2 f_1}{\partial x^2}\right)^2-2\mu\frac{\partial^2 f_1}{\partial x^2}\frac{\partial^2 f_1}{\partial y^2}+2(1+\mu)\left(\frac{\partial^2 f_1}{\partial x\,\partial y}\right)^2\right]dx\,dy \tag{6}$$

$$I_2=\iint f_3\left(\frac{\partial^2 f_1}{\partial x^2}+\frac{\partial^2 f_1}{\partial y^2}\right)dx\,dy \tag{7}$$

$$I_3=\iint\frac{1}{2}\left[\frac{\partial^2 f_1}{\partial y^2}\left(\frac{\partial f_2}{\partial x}\right)^2+\frac{\partial^2 f_1}{\partial x^2}\left(\frac{\partial f_2}{\partial y}\right)^2-2\frac{\partial^2 f_1}{\partial x\,\partial y}\frac{\partial f_2}{\partial x}\frac{\partial f_2}{\partial y}\right] \tag{8}$$

The relation between the twist, the load, and the temperature is obtained by performing the variation on equation (3) with respect to the twist θ with C held constant. The resulting relationship is

$$Db^2(\theta-\theta_i)I_4+2tCb^2\theta I_3-b\iint pf_2\,dx\,dy=0 \tag{9}$$

where

$$I_4=\iint\left[\left(\frac{\partial^2 f_2}{\partial x^2}\right)^2+\left(\frac{\partial^2 f_2}{\partial y^2}\right)^2+2\mu\frac{\partial^2 f_2}{\partial x^2}\frac{\partial^2 f_2}{\partial y^2}+2(1-\mu)\left(\frac{\partial^2 f_2}{\partial x\,\partial y}\right)^2\right]dx\,dy \tag{10}$$

The pressure loading p now will be considered to consist of a static loading p_s and a dynamic or inertia loading $\rho t\,\ddot{w}$ so that

$$p=p_s-\rho t\,\ddot{w} \tag{11}$$

For this analysis the lateral static load p_s will be restricted to two equal concentrated loads P applied at the corners $x=a$, $y=\pm b$ in such a way as to form a couple about the x-axis. Then

$$\iint pf_2\,dx\,dy=\frac{M}{2b}I_5-\rho tb\ddot{\theta}I_6 \tag{12}$$

where

$$I_5=\iint\delta(x-a)[\delta(y-b)-\delta(y+b)]f_2\,dx\,dy \tag{13}$$

$$I_6=\iint f_2^2\,dx\,dy \tag{14}$$

$$M=2bP \tag{15}$$

and δ is the Dirac delta function.

If the value of C from equation (5) is substituted into equation (9) and the terms are rearranged, the resulting expression is

$$b^2(\theta-\theta_i)I_4=\frac{M}{2D}I_5-\rho\frac{tb^2}{D}\ddot{\theta}I_6+\frac{2tb^2\theta}{D}E\alpha\,\Delta T\frac{I_3I_2}{I_1}-\frac{2tb^4}{D}E\theta(\theta^2-\theta_i^2)\frac{(I_3)^2}{I_1} \tag{16}$$

which gives the relationship between twist, applied moment, inertia loading, and temperature.

DEFINITION OF PARAMETERS

It is convenient to define certain parameters which can be obtained from equation (16) when the large-deflection effects are neglected and the initial twist θ_i is 0. Then, from equation (16)

$$b^2\theta I_4=\frac{M}{2D}I_5-\rho\frac{tb^2}{D}\ddot{\theta}I_6+\frac{2tb^2\theta}{D}E\alpha\,\Delta T\frac{I_3I_2}{I_1} \tag{17}$$

If the plate is not vibrating and no loads are applied, the critical, or buckling, temperature difference is obtained from equation (17) as

$$\Delta T_{cr}=\frac{D}{2E\alpha t}\frac{I_1I_4}{I_2I_3} \tag{18}$$

Similarly, when the plate is not vibrating and the temperature is uniform ($\Delta T=0$) but the load is acting, the moment-twist relation is given by

$$\theta=\frac{Ma}{(GJ)_0} \tag{19}$$

where $(GJ)_0$ is the torsional stiffness of the flat plate given by

$$(GJ)_0=2ab^2D\frac{I_4}{I_5} \tag{20}$$

In the absence of heating and loading the frequency may be found to be

$$\omega_0^2=\frac{D}{\rho t}\frac{I_4}{I_6} \tag{21}$$

When equations (18), (19), (20), and (21) are substituted into equation (16) the result may be written as

$$\theta-\theta_i=\frac{Ma}{(GJ)_0}-\frac{1}{\omega_0^2}\ddot{\theta}+\frac{\Delta T}{\Delta T_{cr}}\theta-\theta(\theta^2-\theta_i^2)\frac{2Etb^2}{D}\frac{(I_3)^2}{I_1I_4} \tag{22}$$

If a "nondimensional" twist is defined so that

$$\varphi=\theta\sqrt{\frac{2Etb^2}{D}\frac{(I_3)^2}{I_1I_4}} \tag{23}$$

along with a nondimensional moment

$$m=\frac{Ma}{(GJ)_0}\sqrt{\frac{2Etb^2}{D}\frac{(I_3)^2}{I_1I_4}} \tag{24}$$

and a temperature ratio

$$\lambda=\frac{\Delta T}{\Delta T_{cr}} \tag{25}$$

equation (22) may be written simply as

$$\varphi-\varphi_i=m+\lambda\varphi-\varphi(\varphi^2-\varphi_i^2)-\frac{1}{\omega_0^2}\ddot{\varphi} \tag{26}$$

APPLICATION TO STATIC PROBLEM

The relationship between twist, moment, and temperature is given by equation (26) when the dynamic term $\frac{1}{\omega_0^2}\ddot{\varphi}$ is 0. Equation (26) then becomes

$$\varphi-\varphi_i=m+\lambda\varphi-\varphi(\varphi^2-\varphi_i^2) \tag{27}$$

The incremental stiffness of the plate, defined as the rate of change of moment with respect to twist, is given by

$$\frac{\Delta(GJ)}{(GJ)_0}=\frac{a}{(GJ)_0}\frac{\partial M}{\partial\theta}$$

or, from equation (27),

$$\frac{\Delta(GJ)}{(GJ)_0}=\frac{\partial m}{\partial\varphi}=1-\lambda+3\varphi^2-\varphi_i^2 \tag{28}$$

APPLICATION TO DYNAMIC PROBLEM

In order to determine the effect of temperature, moment, and initial twist on the natural frequency of torsional vibration, the quantity φ in equation (26) is replaced by $\varphi+\epsilon\sin\omega\tau$ where φ is considered to be the static solution obtained from equation (27) and ϵ represents a small dynamic perturbation about the static equilibrium position. Subtracting equation (27) from the perturbated relation, neglecting higher order terms in ϵ, and dividing by $\epsilon\sin\omega\tau$ yields

$$1=\lambda-3\varphi^2+\varphi_i^2+\left(\frac{\omega}{\omega_0}\right)^2$$

The frequency may then be written in terms of the twist and temperature as

$$\left(\frac{\omega}{\omega_0}\right)^2=1-\lambda+3\varphi^2-\varphi_i^2 \tag{29}$$

which is identical to the incremental stiffness (eq. (28)). This identity results from assuming similar deflection mode shapes for thermal buckling, twist due to applied moment, and torsional vibration and would not be expected to apply if the mode shapes involved were different.

RESULTS AND DISCUSSION

GENERAL RESULTS OF EQUATIONS

The behavior of the plate as determined by equation (26) is discussed in the following sections for several combinations of conditions. In most cases the calculations include large values of initial twist and applied moment and have been carried well into the region where the temperature difference ΔT exceeds the critical value. Although some of the results may be beyond the range for which the analysis is accurate, these results have been presented to illustrate the trends indicated by the equations despite the fact that they may not be quantitatively correct in some regions.

Twisting due to an applied moment.—The twisting of the plate due to an applied moment is given by equation (27) if the temperature ratio λ is set equal to 0. The results from this expression are presented in figure 2 for various values of the initial twist.

In figure 2, small-deflection results would plot as lines at 45° to the coordinate axes. The large-deflection results become increasingly different as the moment or initial twist is increased and indicate that the plate becomes substantially stiffer as the twist is increased.

Buckling due to nonuniform heating.—The twist of the plate (assuming that the buckling mode is a twisting action) is given by equation (27) when the moment m is 0; for the initially flat plate φ_i would also be 0. The initially flat, or perfect, plate begins to deform only after the critical temperature difference is reached, whereas, as indicated by equation (27), the plate with initial twist begins to deform immediately upon heating. The results obtained from evaluation of equation (27) are given in figure 3 for several values of the initial twist.

If the initial twist is large, a plot of twist against temperature ratio, like figure 3, does not give an accurate indication of the buckling temperature. Only if the initial twist is small is there a definite knee in the curve as the buckling temperature is approached, but this knee occurs below the buckling temperature of the perfect plate.

Combined action of applied moment and nonuniform heating.—Equation (27) applies directly to this case but may be more conveniently written as

$$\varphi-\varphi'-\lambda'\varphi+\varphi(\varphi^2-\varphi'^2)=0 \tag{30}$$

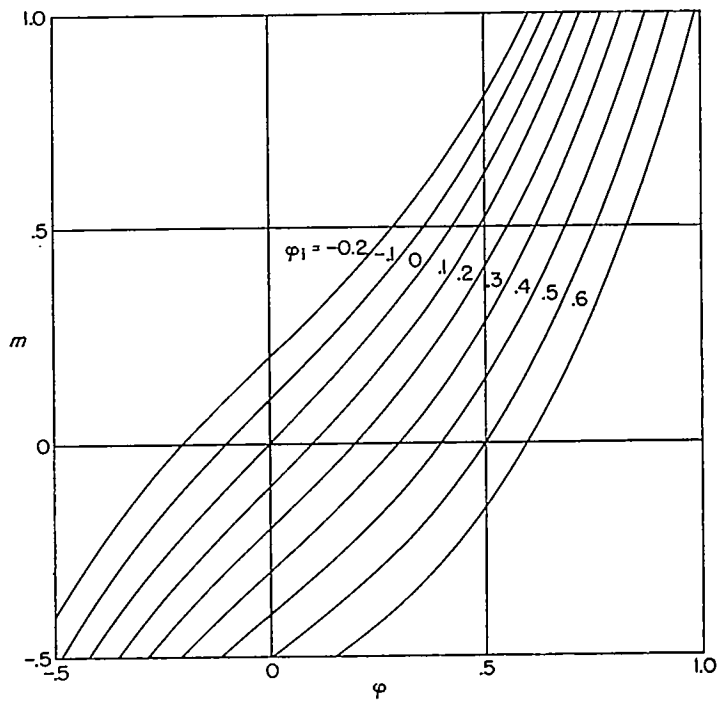

FIGURE 2.—Calculated twist as a function of applied moment for several values of the initial twist.

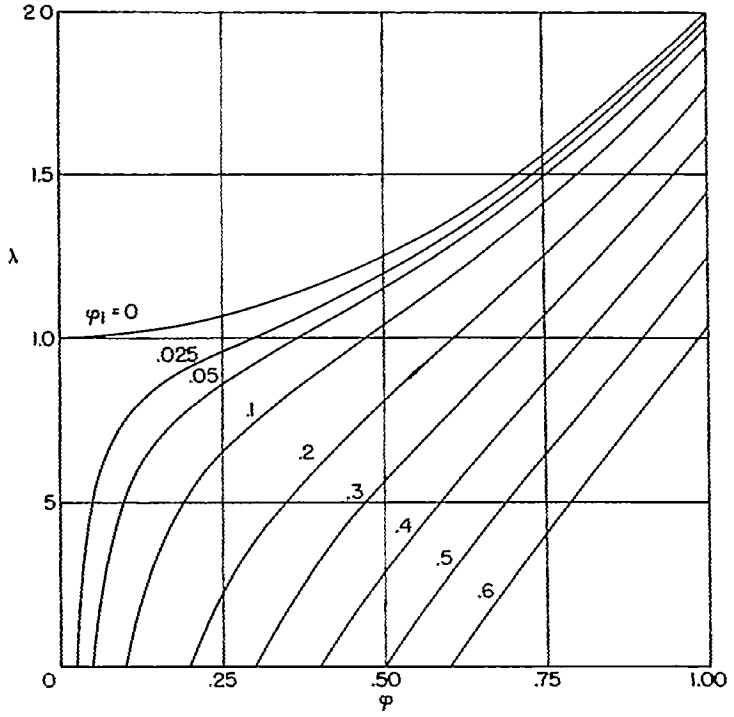

FIGURE 3.—Calculated twist as a function of temperature ratio for several values of initial twist.

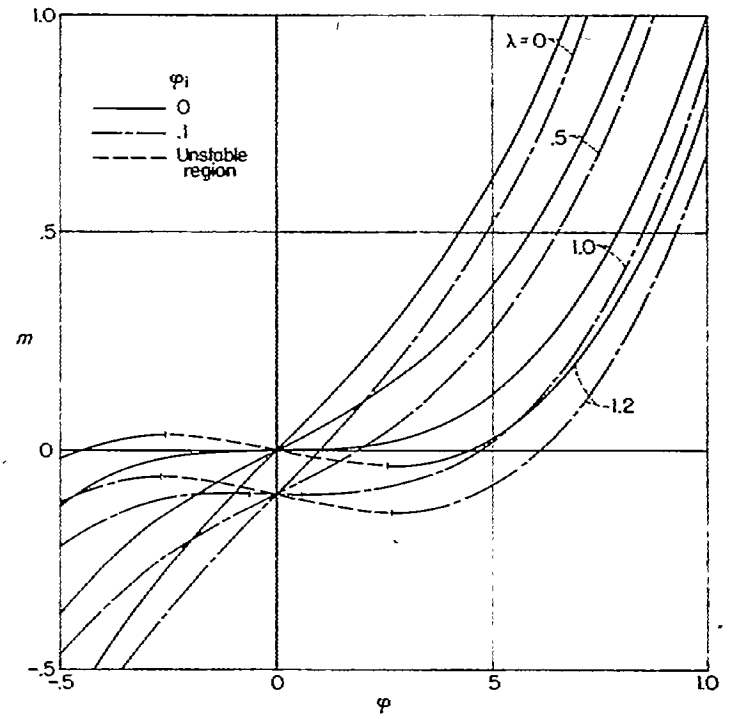

FIGURE 4.—Calculated twist as a function of applied moment for several combinations of temperature ratio and initial twist.

where

$$\varphi' = \varphi_i + m \tag{31a}$$

and

$$\lambda' = \lambda - (m^2 + 2m\varphi_i) \tag{31b}$$

Equation (30) now has the same form as equation (27) when m is set equal to 0. The results plotted in figure 3 then apply to this case also if φ_i is replaced by φ' and λ by λ'. The moment then effectively acts the same as an initial twist if the temperature ratio is reduced by the quantity $m^2+2m\varphi_i$.

In figure 4 the relation between moment and twist has been indicated for two values of initial twist and several values of λ. These curves show the characteristic increase in stiffness as the twist increases but also show a reduction in stiffness as the temperature ratio increases. These changes in stiffness are examined further in the following section. The portions of the curves where the slope is negative have been shown as dashed lines and are regions of unstable equilibrium which would not exist in the physical problem. The unstable portion of the curve exists whenever $\lambda+\varphi_i^2-3\varphi^2>1$.

Frequency and incremental stiffness.—As has been noted, the square of the frequency ratio (eq. (29)) varies in the same manner as the incremental stiffness (eq. (28)) and, therefore, any of the following discussion pertaining to stiffness applies directly to the square of the frequency. Also, the figures which are presented for the incremental stiffness have been labeled with the square of the frequency ratio as well as with the stiffness ratio.

The variation in incremental stiffness with temperature given by equation (28) is shown in figure 5 for several values of initial twist when m is equal to 0. The results show that, when the perfect plate is heated, the stiffness decreases linearly as the thermal stresses develop and becomes zero

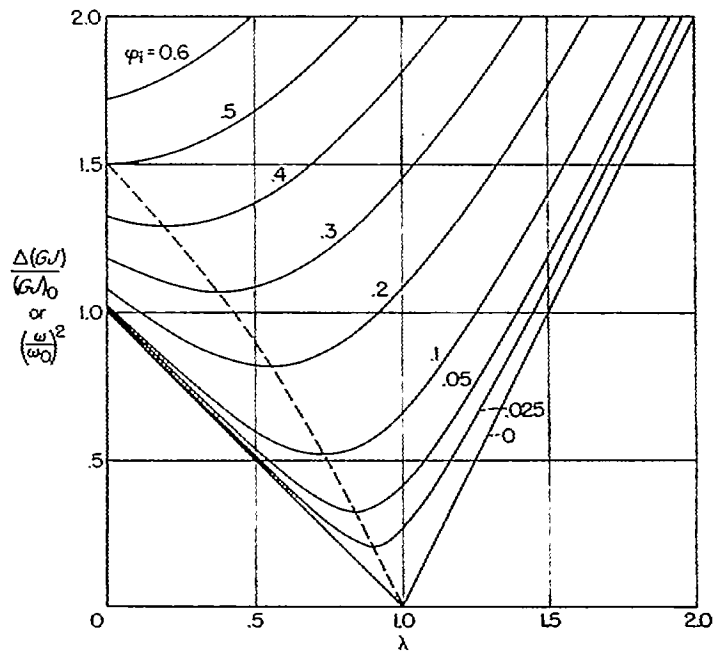

FIGURE 5.—Calculated incremental stiffness as a function of temperature ratio for several values of initial twist.

when the buckling temperature difference is reached Further heating causes the plate to twist and the twisting in turn leads to an increase in stiffness at a rate twice that of the initial decrease.

If the plate has an initial twist, the heating causes the twist to increase as the heating progresses. This twist leads to an increase in stiffness that tends to counteract the reduction produced by thermal stresses and, as a result, the stiffness first decreases and then increases without going to zero. The points of minimum stiffness occur at temperatures lower than the buckling temperature. The locus

of points of minimum stiffness has been indicated in figure 5 by the dashed line. If the initial twist is sufficiently large, the stiffness does not decrease but increases with heating.

When a moment is applied to the plate, figure 5 will indicate the incremental stiffness of the plate if φ_i is replaced by φ' and λ by λ' (as defined by eqs. (31a) and (31b)).

The locus of points where the incremental stiffness is a minimum is given by the equations

$$\frac{\Delta(GJ)_{min}}{(GJ)_0}=6\left(\frac{\varphi_i+m}{4}\right)^{2/3} \tag{32}$$

$$\lambda_{min}=1-\varphi_i^2-3\left(\frac{\varphi_i+m}{4}\right)^{2/3} \tag{33}$$

or

$$\frac{\Delta(GJ)_{min}}{(GJ)_0}=2(1-\lambda_{min}-\varphi_i^2) \tag{34}$$

Equations (33) and (34) show that the nonuniform heating will increase the stiffness of the plate if the initial twist is geater than that given by

$$3\left(\frac{\varphi_i+m}{4}\right)^{2/3}+\varphi_i^2=1$$

The initial incremental stiffness of the plate is given by equation (28) when λ is 0. The ratio of the minimum to the initial incremental stiffness therefore may be written as

$$\frac{\Delta(GJ)_{min}}{\Delta(GJ)_i}=\frac{6\left(\frac{\varphi_i+m}{4}\right)^{2/3}}{1+3\varphi^2-\varphi_i^2} \tag{35}$$

Some results from equation (35) have been plotted in figure 6. This figure indicates that small changes in the initial twist may cause large changes in the minimum incremental stiffness. The effects of applied moment are again similar to those of initial twist and certain combinations of the two can lead to drastic stiffness changes. For negative values of φ_i the curves would be similar, with the stiffness ratio going to zero whenever $\varphi_i=-m$.

COMPARISON WITH EXPERIMENT

Results calculated with the previously derived equations are compared in the following sections with the experimental results reported in reference 5. The results given in reference 5 are for a square cantilever plate which was heated along the two longitudinal edges by carbon-rod radiators. Typical temperature histories of points on the heated edge and on the longitudinal center line are given in figure 7. Heat was supplied to the plate edges for 16 seconds; then the plate was allowed to cool. The deformations of the plate under the influence of nonuniform heating were determined for the conditions of no load and applied positive and negative tip moments. The changes in natural frequency of the first torsion mode were also measured during a heating test.

The expressions used in reference 5 for stresses, deflections, and temperature are retained except that herein only

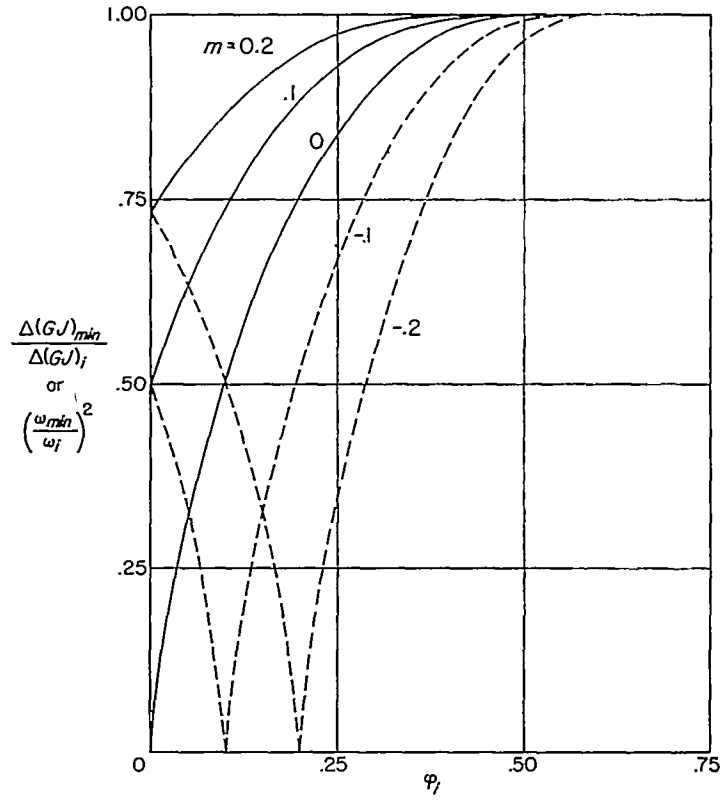

FIGURE 6.—Calculated ratio of minimum incremental stiffness to initial incremental stiffness as a function of initial twist for several values of applied moment.

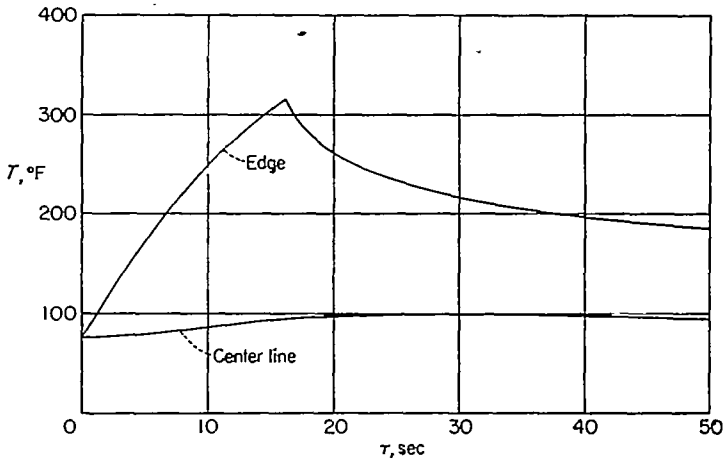

FIGURE 7.—Measured temperature histories for a heated edge and the center line of the plate test specimen.

three terms are used for the deflections. In nondimensional form these expressions are

$$f_1=\left[\left(\frac{x}{a}\right)^2-1\right]^2\left[\left(\frac{y}{b}\right)^2-1\right]^2 \tag{36}$$

$$f_2=\frac{\frac{y}{b}\left[\left(\frac{x}{a}\right)^2+A_1\left(\frac{x}{a}\right)^3+A_2\left(\frac{x}{a}\right)^4\right]}{1+A_1+A_2} \tag{37}$$

and

$$f_3=\left(\frac{y}{b}\right)^5 \tag{38}$$

The function f_1 satisfies the condition of zero stress on the free edges and f_2 specifies zero slope and deflection along the root. The two undetermined coefficients of equation (37) are established from the small-deflection buckling analysis and carried through the large-deflection analysis as constants. Their values are given in appendix A along with data on the influence of the number of terms in the deflection function on the accuracy with which the buckling temperature difference, natural frequency, and ratio of twist to an applied moment can be calculated. The exponential parameter ζ of the temperature function is adjusted to approximate the variation in the temperature distribution during a test.

The numerical evaluation of the integrals and related functions required for comparison of theory and experiment are given in appendix B.

Initial plate shape.—The initial shape of the plate of reference 5 was measured and is indicated in figure 8. In the selection of a value of initial twist, the higher order shapes (which are unlikely to have much influence on the twisting) have been ignored. The free corners were connected by a straight line in order to obtain a value of initial twist of $\theta_i=0.35°$ which was used for comparison of theory and experiment.

Twist due to an applied moment.—The deformations resulting from heating for three values of applied tip moment are presented in figure 9 and compared with curves calculated by use of a value of $\theta_i=0.35°$. The agreement between theory and experiment is satisfactory, although the theory overestimates the twist in the vicinity of the maximum temperature difference (about 16 seconds). No theoretical results are presented past 20 seconds because, beyond this time, the actual temperature distribution cannot be represented very well by the one-parameter temperature function.

Another comparison of measured and calculated deformations is shown in figure 10 where the abscissa is the temperature difference instead of time. Because the shape of the temperature distribution changes with time, the portion of the curve for decreasing ΔT does not retrace the heating portion.

Natural frequency.—The changes in natural frequency during a heating test are shown in figure 11 and compared

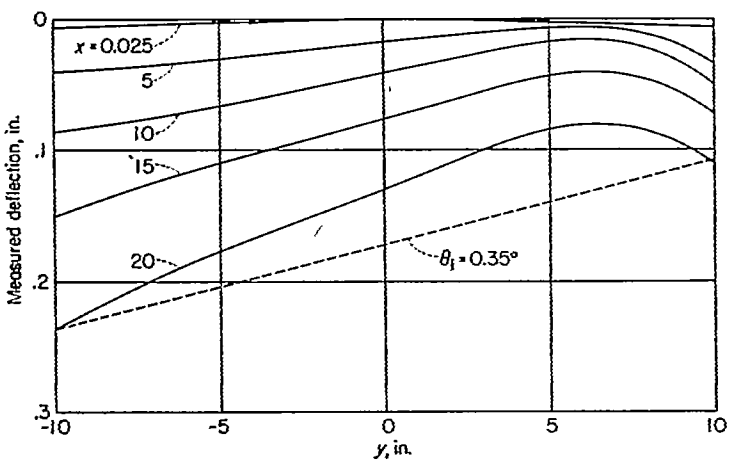

FIGURE 8.—Initial shape of plate test specimen.

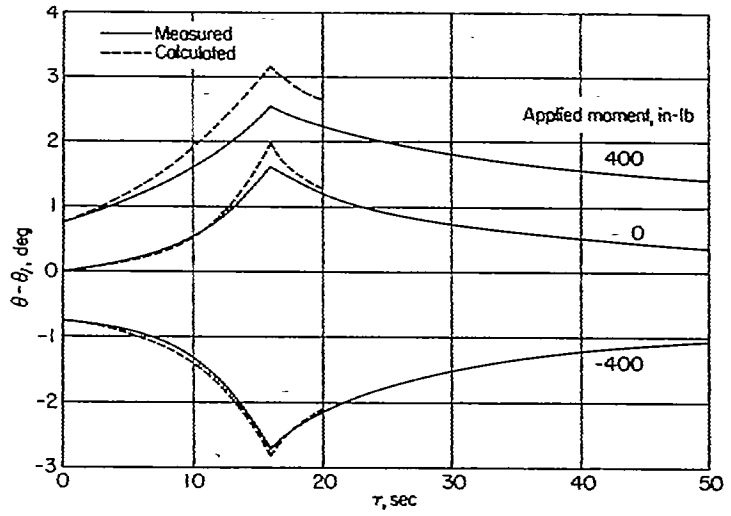

FIGURE 9.—Comparison of measured and calculated values of twist as a function of time for the rapidly heated plate for three values of applied moment.

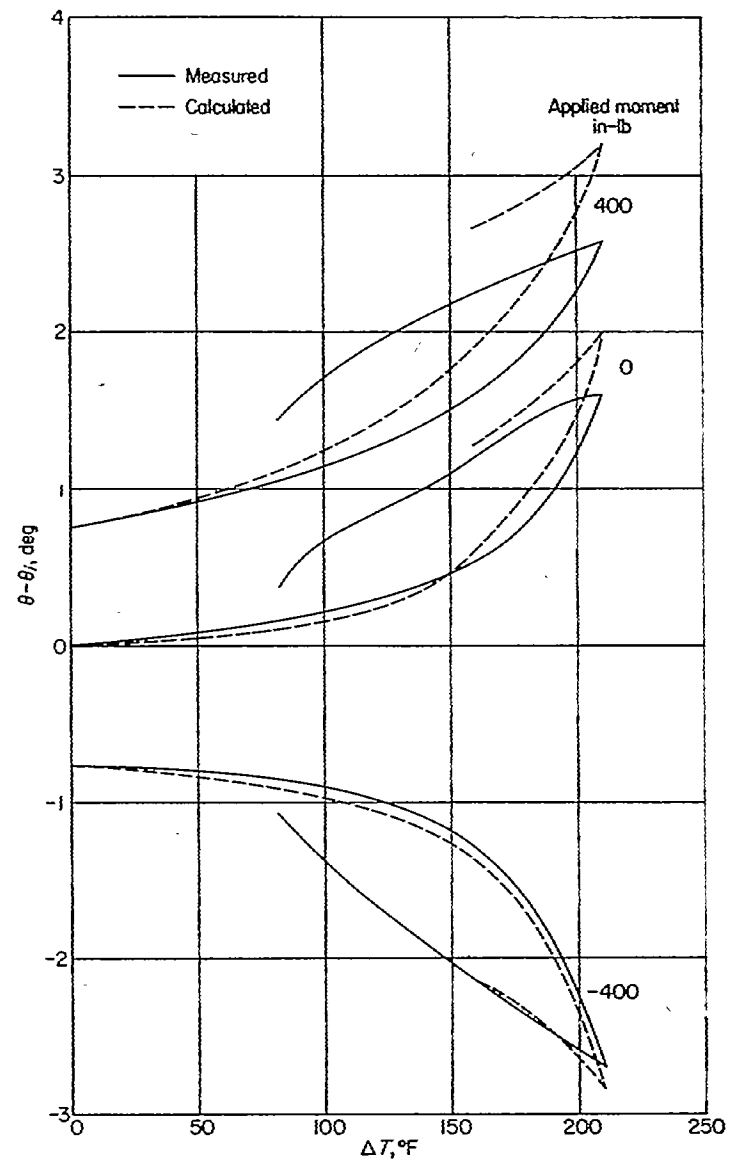

FIGURE 10.—Comparison of measured and calculated values of twist as a function of temperature difference for three values of the applied moment.

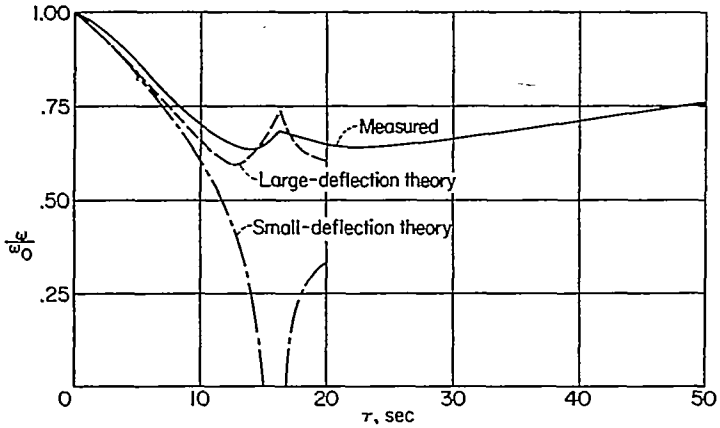

FIGURE 11.—Comparison of measured and calculated values of frequency ratio as a function of time for the rapidly heated plate.

with a calculated curve for $\theta_i=0.35°$ and with the small-deflection results of reference 5. The results calculated by the use of the large-deflection equations are in good agreement with experimental values and account for the frequency increase measured in the vicinity of the buckling temperature. A substantial improvement is noted over the predictions of small-deflection theory. In figure 12 the frequency ratio is shown as a function of temperature difference.

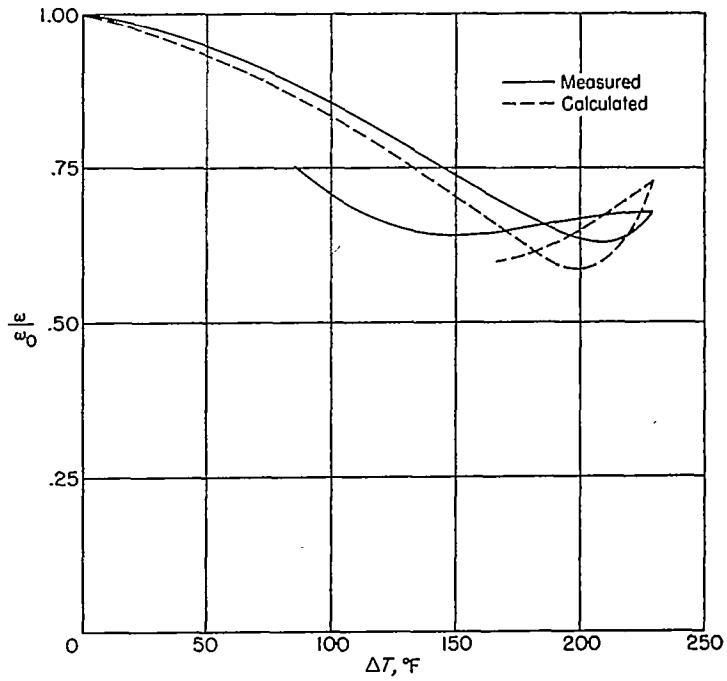

FIGURE 12.—Comparison of measured and calculated values of the frequency ratio as a function of temperature difference.

CONCLUDING REMARKS

An approximate analysis of the effects of initial twist and large deflections on the torsional stiffness of a cantilever plate subjected to nonuniform heating shows that for a perfectly flat plate the effective stiffness, and thus the torsional frequency, decreases with increasing thermal stress, just as predicted by small-deflection theory, and goes to zero when the buckling temperature difference is reached. Beyond the buckling temperature, however, the stiffness, and thus the frequency, increases as the plate twists. If the plate has an initial twist, it begins to deform immediately upon heating and the stiffness decreases in much the same way as that of the perfect plate. The incremental stiffness of the initially twisted plate, however, reaches a minimum greater than zero before the theoretical buckling temperature difference is reached; further heating then increases the stiffness. The minimum incremental stiffness is a function of the initial twist and, if the initial twist is sufficiently large, no reductions in stiffness are obtained and nonuniform heating then always increases the stiffness.

These results for stiffness changes associated with the torsional frequency are also applicable to the stiffness of the plate with respect to small changes in the applied moment. In this case the applied moment has an effect similar to the effect of an initial twist. If the applied moment exactly counteracts the initial twist, the plate behaves in much the same way as the perfect plate.

Calculated results were compared with available experimental data and were found to be in satisfactory agreement in view of the approximate nature of the calculations.

LANGLEY AERONAUTICAL LABORATORY,
NATIONAL ADVISORY COMMITTEE FOR AERONAUTICS,
LANGLEY FIELD, VA., *May 15, 1957.*

APPENDIX A

DISCUSSION OF MODAL FUNCTIONS USED IN THE ANALYSIS

In the analysis of the torsional deformations of the cantilever plate by small-deflection theory, a deflection function containing six terms antisymmetrical in the coordinate y was used. The function (eq. (8) in ref. 5) is

$$w=A_{12}x^2y+A_{14}x^2y^3+A_{22}x^3y+A_{24}x^3y^3+A_{32}x^4y+A_{34}x^4y^3 \qquad \text{(A1)}$$

The effect of various combinations of terms on the calculated critical temperature difference, torsional frequency, and moment-twist relation was investigated for a square cantilever plate ($a/b=2$) by use of the small-deflection theory of reference 5. The following table shows the results obtained by starting with a single term A_{12} and then progressing through other combinations to six terms:

Terms used	$\frac{\Delta T_{cr}}{K_1}$	$\frac{\omega_0^2}{K_2}$	$\frac{M}{\theta}$
A_{12}	103.9	127.0	0.324×10^5
A_{12}, A_{22}	57.7	77.5	.278
A_{12}, A_{22}, A_{32}	50.4	71.3	.273
A_{12}, A_{22}, A_{14}, A_{24}	57.2	77.4	.278
A_{12}, A_{22}, A_{32}, A_{14}, A_{24}, A_{34}	50.0	70.1	.273

where K_1 and K_2 represent constants that include the plate dimensions and material properties.

Inasmuch as the tabulated values were obtained from an application of the Rayleigh-Ritz procedure, the lowest value is the most accurate. The use of six terms improves the accuracy less than 2 percent over three terms and, consequently, is not worth the extra complication. The large-deflection analysis thus can be made by use of only three terms. The deflection function is nondimensionalized for this analysis and expressed in the form

$$f_2=\frac{\frac{y}{b}\left[\left(\frac{x}{a}\right)^2+A_1\left(\frac{x}{a}\right)^3+A_2\left(\frac{x}{a}\right)^4\right]}{1+A_1+A_2} \qquad \text{(A2)}$$

The relative values of these coefficients for the conditions given in the preceding table were obtained from the small-deflection analysis of reference 5 for the square cantilever plate ($a/b=2$) with the following results:

Condition	$\frac{1}{1+A_1+A_2}$	$\frac{A_1}{1+A_1+A_2}$	$\frac{A_2}{1+A_1+A_2}$
Thermal buckling ($\lambda=1$, $\omega/\omega_0=0$)	4.61	−5.75	2.14
Torsional vibration ($\lambda=0$, $\omega/\omega_0=1$)	3.63	−4.06	1.42
Applied moment ($\lambda=0$)	2.36	−2.01	0.65
Applied moment ($\lambda=0.5$)	3.10	−3.20	1.10

The variation of f_2 with x/a for these four conditions has been plotted in figure 13. The table indicates a wide variation in the relative values of the coefficients but the plotted data show that the deflection shapes are all approximately the same. Then, so long as the calculations are used to indicate changes from the initial conditions, any of the modes indicated should be satisfactory.

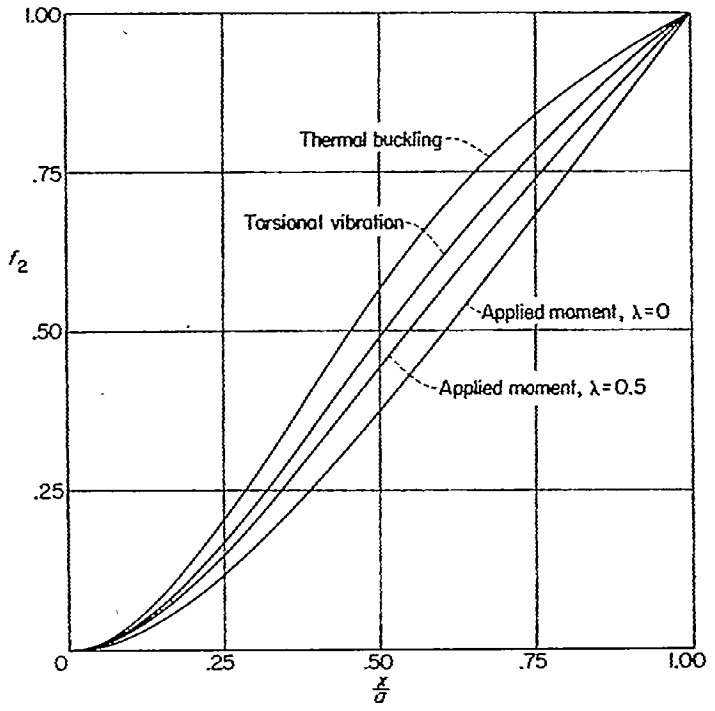

FIGURE 13.—Comparison of deflected shapes for thermal buckling, torsional vibration, and twist due to an applied moment as given by small-deflection theory.

In addition to the deflection function of equation (A2), a stress function and a temperature function are required in the analysis and have been selected to correspond to those of reference 5. For convenience, the functions are expressed in nondimensional form as follows:

$$f_1=\left[\left(\frac{x}{a}\right)^2-1\right]^2\left[\left(\frac{y}{b}\right)^2-1\right]^2 \qquad \text{(A3)}$$

$$f_3=\left(\frac{y}{b}\right)^\zeta \qquad \text{(A4)}$$

The exponent ζ must be selected to describe best the measured temperature distribution at the time of interest. Note that equation (A4) requires that the specified temperature difference ΔT be the difference between temperatures at the heated edges and the longitudinal center line. The function f_1 has been chosen so that the stresses vanish on the free boundaries. Along the root ($x=0$) the function requires that the plate be free to expand parallel to the y-axis. Although this requirement does not indicate a "built-in" condition, it probably resembles the actual test condition.

APPENDIX B

EVALUATION OF INTEGRALS AND RELATED FUNCTIONS

The integrals indicated in the analysis have been evaluated in terms of the plate dimensions and the nondimensional functions given in appendix A. The integrals are as follows:

$$I_1=\int_0^a\int_{-b}^b\left[\left(\frac{\partial^2 f_1}{\partial y^2}\right)^2+\left(\frac{\partial^2 f_1}{\partial x^2}\right)^2-2\mu\frac{\partial^2 f_1}{\partial x^2}\frac{\partial^2 f_1}{\partial y^2}+2(1+\mu)\left(\frac{\partial^2 f_1}{\partial x\,\partial y}\right)^2\right]dx\,dy=\left(\frac{128}{105}\right)^2\frac{b}{a^3}\left[7\left(\frac{a}{b}\right)^4+4\left(\frac{a}{b}\right)^2+7\right] \tag{B1}$$

$$I_2=\int_0^a\int_{-b}^b f_3\left(\frac{\partial^2 f_1}{\partial x^2}+\frac{\partial^2 f_1}{\partial y^2}\right)dx\,dy=\frac{128}{15}\frac{a}{b}\frac{\zeta}{(\zeta+3)(\zeta+1)} \tag{B2}$$

$$I_3=\int_0^a\int_{-b}^b\frac{1}{2}\left[\frac{\partial^2 f_1}{\partial y^2}\left(\frac{\partial f_2}{\partial x}\right)^2+\frac{\partial^2 f_1}{\partial x^2}\left(\frac{\partial f_2}{\partial y}\right)^2-2\frac{\partial^2 f_1}{\partial x\,\partial y}\frac{\partial f_2}{\partial x}\frac{\partial f_2}{\partial y}\right]dx\,dy$$
$$=\frac{128}{15ab(1+A_1+A_2)^2}\left(\frac{4}{105}+\frac{A_1^2}{35}+\frac{16A_2^2}{693}+\frac{A_1}{16}+\frac{16A_2}{315}+\frac{A_1A_2}{20}\right) \tag{B3}$$

$$I_4=\int_0^a\int_{-b}^b\left[\left(\frac{\partial^2 f_2}{\partial x^2}\right)^2+\left(\frac{\partial^2 f_2}{\partial y^2}\right)^2+2\mu\left(\frac{\partial^2 f_2}{\partial x^2}\frac{\partial^2 f_2}{\partial y^2}\right)+2(1-\mu)\left(\frac{\partial^2 f_2}{\partial x\,\partial y}\right)^2\right]dy\,dx=\frac{b}{a^3(1+A_1+A_2)^2}\left[\frac{8}{3}+8A_1^2+\frac{96}{5}A_2^2+8A_1+\frac{32A_2}{3}+24A_1A_2+2(1-\mu)\left(\frac{a}{b}\right)^2\left(\frac{8}{3}+\frac{18A_1^2}{5}+\frac{32A_2^2}{7}+6A_1+\frac{32A_2}{5}+8A_1A_2\right)\right] \tag{B4}$$

$$I_5=\int_0^a\int_{-b}^b\delta(x-a)\,[\delta(y-b)-\delta(y+b)]f_2\,dy\,dx=2 \tag{B5}$$

$$I_6=\int_0^a\int_{-b}^b f_2^2\,dy\,dx=\frac{2ab}{3(1+A_1+A_2)^2}\left(\frac{1}{5}+\frac{A_1^2}{7}+\frac{A_2^2}{9}+\frac{A_1}{3}+\frac{2A_2}{7}+\frac{A_1A_2}{4}\right) \tag{B6}$$

For the square cantilever plate ($a/b=2$) and the values of A_1 and A_2 given in appendix A for the thermal-buckling mode, the integrals I_1 to I_4 reduce to the following when Poisson's ratio μ equals 0.33:

$$I_1=\left(\frac{128}{105}\right)^2\frac{135}{2a^2} \tag{B7}$$

$$I_2=\frac{256}{15}\frac{\zeta}{(\zeta+3)(\zeta+1)} \tag{B8}$$

$$I_3=\frac{1.520}{a^2} \tag{B9}$$

$$I_4=\frac{9.567}{a^2} \tag{B10}$$

The integrals I_5 and I_6 have not been included but are discussed subsequently.

The critical temperature difference given by equation (18) then becomes

$$\Delta T_{cr}=18.5\frac{D}{E\alpha t a^2}\left[\frac{(\zeta+1)(\zeta+3)}{\zeta}\right] \tag{B11}$$

The twist and applied moment are related to their corresponding nondimensional quantities by equations (23) and (24) and may now be expressed as

$$\varphi=0.035\theta\sqrt{\frac{Eta^2}{D}} \tag{B12}$$

$$m=0.035\frac{Ma}{(GJ)_0}\sqrt{\frac{Eta^2}{D}} \tag{B13}$$

Use of the thermal-buckling mode yields incorrect values for the natural frequency and the twist due to applied moment. In addition, the measured values differ slightly from the correct calculated values as a result of the imperfect clamping at the root of the cantilever plate. For these reasons, the measured initial values of torsional frequency and twist due to an applied moment are used in the calculations and the changes produced by the heating cycle are calculated from the following equations:

$$\lambda=1-\frac{\varphi_i+m}{\varphi}+\varphi^2-\varphi_i^2 \tag{B14}$$

$$\left(\frac{\omega}{\omega_0}\right)^2=1-\lambda+3\varphi^2-\varphi_i^2 \tag{B15}$$

The integrals I_5 and I_6 are needed only to calculate the initial natural frequency and twist due to applied moment and, thus, have not been evaluated for the mode shape of thermal buckling.

In the calculations, results of which are presented in figures 9, 10, 11, and 12, the following quantities were used:

$E=10.6\times10^6$ psi
$\alpha=12.8\times10^{-6}$ °F^{-1}
$\mu=0.33$
$t=0.25$ in.
$a=20$ in.
$b=10$ in.
$\theta_i=0.35°$

REFERENCES

1. Dryden, Hugh L., and Duberg, John E.: Aeroelastic Effects of Aerodynamic Heating. Proc. of the Fifth AGARD General Assembly (Canada), June 15–16, 1955, pp. 102–107.
2. Bisplinghoff, R. L.: Some Structural and Aeroelastic Considerations of High-Speed Flight—The Nineteenth Wright Brothers Lecture. Jour. Aero. Sci., vol. 23, no. 4, Apr. 1956, pp. 289–329, 367.
3. Heldenfels, Richard R., and Roseerans, Richard: Preliminary Results of Supersonic-Jet Tests of Simplified Wing Structures. NACA RM L53E26a, 1953.
4. Budiansky, Bernard, and Mayers, J.: Influence of Aerodynamic Heating on the Effective Torsional Stiffness of Thin Wings. Jour. Aero. Sci., vol. 23, no. 12, Dec. 1956, pp. 1081–1093, 1108.
5. Vosteen, Louis F., and Fuller, Kenneth E.: Behavior of a Cantilever Plate Under Rapid-Heating Conditions. NACA RM L55E20c, 1955.
6. Gossard, Myron L., Seide, Paul, and Roberts, William M.: Thermal Buckling of Plates. NACA TN 2771, 1952.
7. Reissner, Eric: On a Variational Theorem for Finite Elastic Deformations. Jour. Math. and Phys., vol. XXXII, nos. 2–3, July-Oct. 1953, pp. 129–135.